Plasma Chemistry and Plasma Processing (2025) 45:1–20
https://doi.org/10.1007/s11090-024-10529-w

ORIGINAL PAPER

Separation of Plasma Species for Investigating the Impact of Hydrogen Plasmas on the Work Function of Caesiated Surfaces

A. Heiler[1] · **R. Friedl**[2] · **U. Fantz**[1,2]

Received: 30 August 2024 / Accepted: 29 October 2024 / Published online: 2 December 2024

Abstract
In negative hydrogen ion sources in situ adsorption of Cs is typically used to generate low work function converter surfaces. The achievement of a temporally stable low work function coating is, however, challenging due to the hydrogen plasma interaction with the surface. Particularly in ion sources for neutral beam injection systems for fusion with pulse durations of minutes to hours temporal instabilities are a major issue and limit the source performance. To clarify the influence of the hydrogen plasma on the converter surface, investigations are performed at an experiment equipped with an absolute work function diagnostic based on the photoelectric effect. Caesiated surfaces are exposed to the full plasma impact by the generation of plasmas in front of the surface as well as to selected plasma species (H atoms, positive ions and VUV/UV photons) from an external plasma source to identify driving mechanisms that lead to surface changes. Depending on the exposure time and initial surface condition, the plasma strongly affects the surface in terms of work function and quantum efficiency (QE). For degraded Cs layers (work function ≥ 3 eV) a favorable increase in QE and reduction in work function can be achieved, while for Cs layers with an ultra-low work function of $1.2 - 1.3$ eV the opposite is true. It is found that each plasma species can influence the Cs layers and that VUV photons lead to a work function increase of ultra-low work function layers. For sufficiently high VUV fluences a severe work function increase by 0.5 eV is given, highlighting the relevance of photochemical processes in the plasma-surface interaction and demonstrating that ultra-low work function layers are not stable in a hydrogen plasma environment.

Keywords Negative hydrogen ion source · Neutral beam injection · Plasma-surface interaction · Caesium · Work function

✉ A. Heiler
adrian.heiler@ipp.mpg.de

[1] Max-Planck-Institut für Plasmaphysik, Boltzmannstrasse 2, D-85748 Garching, Germany

[2] AG Experimentelle Plasmaphysik, Universität Augsburg, D-86135 Augsburg, Germany

Introduction

Negative hydrogen ion sources for fusion and accelerators predominantly rely on the surface production of negative ions on the extraction electrode (converter surface) [1–3]. The surface production represents an electron transfer process from the converter surface to impinging hydrogen atoms and positive ions, which are generated in a low pressure hydrogen plasma in the ion source. The converter surface is typically made of Mo and has a work function of $4.3 - 4.6$ eV [4–6]. As the conversion efficiency for negative ions is higher the lower the work function, the alkali metal Cs is evaporated into the source [1, 7–9]. Cs exhibits a bulk work function of $2.0 - 2.1$ eV (lowest of all stable elements) and its adsorption on surfaces enables a drastic reduction in the work function [4–6, 10, 11]. However, the usage of Cs introduces temporal dynamics, since Cs is volatile, highly reactive and interacts with several species present in the ion source. Among them are reactive hydrogen atoms (radicals), positive hydrogen ions, and energetic vacuum-ultraviolet (VUV) photons with energies up to 15 eV [12–14]. The VUV radiation results mainly from resonant molecular and atomic transitions (molecular Lyman and Werner bands and atomic Lyman series) and the occurring fluxes can be comparable to the positive ion flux [14, 15]. Furthermore, the plasma-surface interaction leads to an effective redistribution of Cs within the source, where most of the Cs is ionized and Cs self-sputtering can occur [16, 17]. In addition, impurities play a decisive role in the Cs layer formation in vacuum phases between pulses because ion sources typically operate under non-ultra-high vacuum conditions [18]. In consequence, the multitude of physico-chemical interactions can change the chemical composition at the surface over time and thus the work function of the converter surface resulting in a variation of the negative ion production rate.

Recent measurements revealed that caesiation under moderate vacuum conditions allows the formation of temporally stable Cs layers with a work function of 1.25 ± 0.10 eV [19, 20]. The ultra-low work function has already been proven in the ion source of the BATMAN Upgrade (BUG) test facility (base pressure 5×10^{-7} mbar) and is attributed to the formation of Cs oxides upon interaction of Cs with residual water [21]. When the Cs evaporation into the source is low or stopped, however, the impurity gases lead to a gradual degradation of the Cs layer and the work function increases to values above 3 eV [19, 20]. Therefore, the Cs layer needs to be conditioned in a suitable manner. First investigations at BUG demonstrated that the extracted ion current strongly depends on the work function evolution of the converter surface, and since the electron density close to the extraction system depends on the negative ion density due to the quasineutrality condition, the work function is also decisive for the co-extracted electron current [21]. The co-extracted electron current typically increases over time during long pulse operation and can limit the achievable ion source performance with respect to the extracted negative ion current [22, 23]. Hence, a detailed understanding of how the hydrogen plasma affects the work function of the converter surface is of utmost importance for the optimization of the ion source and its Cs management.

To study the impact of the hydrogen plasma interaction with caesiated surfaces, investigations are carried out at a dedicated laboratory experiment equipped with an absolute work function diagnostic. The surfaces are selectively exposed to VUV photons, hydrogen atoms and/or positive hydrogen ions in order to reveal driving forces for surface changes upon the plasma-surface interaction. The selective exposure is realized by the application of an external plasma source attached to the experiment. In addition, plasmas can be generated in front of the surface to study the impact of the full plasma-surface interaction on

the surface. The experimental setup is described in Sec. 2 and results on the impact of the specific plasma species and full plasma exposure on the work function are presented in Sec. 3, where it is distinguished between starting from degraded Cs layers in 3.1 and ultra-low work function layers in 3.2. A compilation of the found work function dynamics is provided in Sec. 3.3 and conclusions for negative hydrogen ion sources are given in Sec. 4.

Experiment

Experiments are carried out at ACCesS, which is a planar inductively coupled plasma (ICP) experiment dedicated to work function investigations [19, 24–26]. The setup consists of a water-cooled stainless steel vacuum vessel (15 cm inner diameter, 10 cm height) that is evacuated with a rotary vane and turbomolecular pump to a background pressure of some 10^{-6} mbar (limited by Viton O-ring seals). The background pressure is measured with a cold cathode gauge and the composition of the residual gas is monitored with a differentially pumped residual gas analyzer (RGA), showing that water is the main residual gas. As can be seen in Fig. 1, a sample holder is installed close to the center of the vessel, where Cu samples ($30 \times 30 \times 5\ \mathrm{mm}^3$) with a 3 µm polycrystalline Mo coating are mounted within this work. The samples are mounted electrically and thermally insulated from the chamber walls and the temperature of the sample surface is monitored with a thermocouple. Gas supply is provided by mass flow controllers and low pressure plasmas (several Pa) can be ignited by means of a planar solenoid on top of the vessel (not shown in Fig. 1), separated from the vacuum by a Borosilicate glass plate and connected to a radio frequency (RF) generator (27.12 MHz, 600 W max.).

The absolute work function of the surface installed at the sample holder is measured photoelectrically after the Fowler method [27]. The surface is irradiated with photon energies in the range of $\epsilon_{\mathrm{ph}} = 5.04 - 1.45$ eV, for which a high pressure mercury lamp in

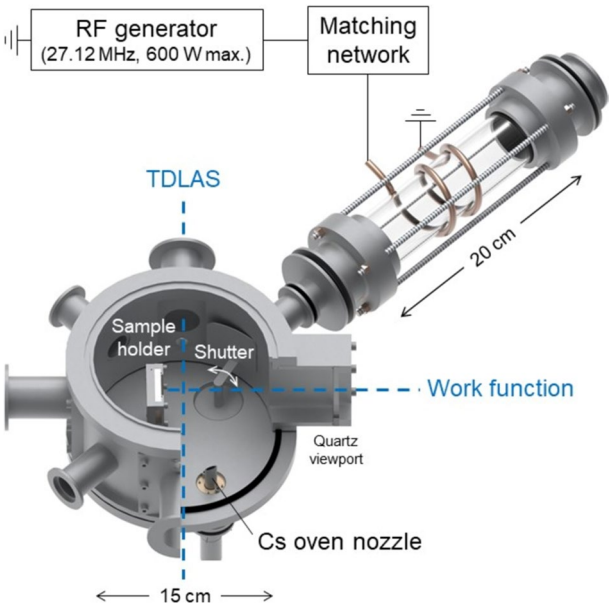

Fig. 1 Sectional view of the ACCesS experiment, upgraded by an external ICP source. The line-of-sights of the tunable diode laser absorption spectroscopy (TDLAS) and work function diagnostic are indicated by blue dashed lines

combination with 20 interference filters (10 nm FWHM) is used. The light is focused with quartz lenses and guided through a quartz viewport onto the surface, resulting in a spot diameter of about 15 mm and radiant powers of $P_{ph} \sim 0.1 - 1$ mW. The photoemitted electrons are drawn to the grounded vessel walls with a bias of −30 V applied to the sample and the resulting photocurrents $I_{ph}(\epsilon_{ph})$ are measured with a picoammeter (dark current typically in the range of $10^{-11} - 10^{-10}$ A). The photocurrents are converted to quantum efficiencies by

$$QE = \frac{\epsilon_{ph} I_{ph}}{e P_{ph}}, \tag{1}$$

and are fitted according to [27]

$$QE \propto T_{surf}^2 \int_0^\infty \ln[1 + \exp(-y + \kappa)]dy \tag{2}$$

to evaluate the work function χ, with $\kappa := (\epsilon_{ph} - \chi)/(k_B T_{surf})$, and e, k_B and T_{surf} denoting the electron charge, Boltzmann constant and measured surface temperature. One work function measurement takes about 2 min and is possible only during plasma-off phases. The typical uncertainty of the evaluated work function is ±0.1 eV. More details about the work function diagnostic can be found in Ref. [19].

To deposit Cs on the sample surface, a Cs oven is attached to the bottom plate of the vacuum chamber. The Cs oven contains a liquid Cs reservoir (1 g Cs ampoule) that is heated to finely adjust the Cs evaporation rate [28], and the Cs oven nozzle is directed toward the sample holder. The density of neutral Cs atoms in the gas phase is measured line-of-sight (LOS) averaged by means of a tunable diode laser absorption spectroscopy (TDLAS) system [29]. The LOS has a diameter of 8 mm and is parallel to and at a distance of 2 cm from the sample surface. With an absorption length of 15 cm the lower detection limit of the neutral Cs density is $n_{Cs} \approx 10^{13}$ m^{-3}. The temperature of the Cs atoms T_{Cs} can be evaluated from the absorption line profile, as it is dominated by Doppler broadening and well approximated by a Gaussian fit [29, 30]. Under the assumption of an isotropic thermal distribution of velocities, the neutral Cs flux onto the sample is calculated via $\Gamma_{Cs} = n_{Cs}\bar{v}_{Cs}/4$, with $\bar{v}_{Cs} = (8k_B T_{Cs}/(\pi m_{Cs}))^{0.5}$ being the mean thermal velocity of the Cs atoms.

Separation of Plasma Species Fluxes

To expose the caesiated surfaces selectively to hydrogen plasma species, an external ICP source is attached to the ACCesS main chamber as shown in Fig. 1. The external plasma source is connected to a flange whose cylinder axis forms an angle of 45° to the normal of the surface. The external plasma source consists of a cylindrical quartz glass tube, which has an inner diameter of 43 mm and a length of 200 mm. Pumping and gas feeding is done via the main chamber and is monitored by a pressure gauge at the back end of the external plasma source. By using a helical two-turn copper coil powered by the 27.12 MHz RF generator, low pressure plasmas are generated. The quartz tube is air cooled to limit its temperature increase to about 150 − 200 °C during steady-state operation. A grounded stainless steel mesh is inserted inside the connection flange to the main chamber to prevent capacitive plasma ignition in the main chamber. The flange opening can be covered with a

rotatable shutter installed in the main chamber, which is used to prevent Cs diffusion into the flange during caesiation.

To select the hydrogen plasma species entering the main chamber, magnetic and optical filters are applied.

VUV Photons + Atoms + Positive Ions

Photons together with hydrogen atoms and positive hydrogen ions can reach the caesiated surface when no filter is applied. Since the photons have energies up to 15 eV, the surface is exposed to energetic VUV irradiation.

VUV Photons + Atoms

To down-select the interacting species with the surface, positive hydrogen ions are deflected by a magnetic filter field. The magnetic field is created by permanent magnets outside the connection flange, leading to a Larmor radius of the order of mm (magnetic flux density $\sim$ 100 mT inside the flange). Since the Larmor radius is much smaller than the experimental dimensions, the ions are magnetized and cannot reach the surface in the main chamber.

VUV Photons

To separate photons from hydrogen atoms and ions, a MgF_2 window is installed inside the connection flange. The MgF_2 window serves as long pass filter with a cut-on wavelength in the VUV at 113 nm (11.0 eV), i.e., the photon energies are somewhat limited compared to the previous two configurations. The transmission of the window is 93% (tested up to 700 nm) and starts to decrease for wavelengths below 200 nm. As the transmission is still 69% at 120 nm, VUV photons from the intense Lyman-α line (121.6 nm), Lyman band ($130 - 170$ nm) and partly from the Werner band ($80 - 130$ nm) can pass through the window. The mount of the MgF_2 window is not vacuum tight so that pumping and gas feeding of the external plasma source can still be done via the main chamber.

Quantification of Plasma Species Fluxes

To determine absolute VUV fluxes generated in the external plasma source, an in-house developed VUV diagnostic is used, which is described in detail in Ref. [31]. The diagnostic is based on a VUV sensitive photodiode and optical filters for wavelength selection. The selected ranges are $6.6 - 8.4$ eV for the dominant emission of the molecular Lyman band, $9.6 - 10.8$ eV for the dominant atomic Lyman-α line at 10.2 eV, and $\geq$ 11.0 eV for the molecular Werner band and atomic Lyman series beyond Lyman-α. By installing the VUV diagnostic at the back end of the external plasma source, VUV emissivities are measured from a viewing cone along the cylinder axis of the quartz tube. The corresponding VUV fluxes leaving the plasma volume are determined from the measured emissivities by multiplication with the volume to surface ratio of the plasma, i.e., homogeneous and isotropic emission within the plasma is assumed [31].

The fluxes of hydrogen atoms and positive hydrogen ions leaving the external plasma source are determined from the thermal flux ($\Gamma_H \propto n_H \sqrt{T_{gas}}$) and Bohm flux ($\Gamma_i \propto n_e \sqrt{T_e/m_i}$), respectively. To measure the required plasma parameters, optical

emission spectroscopy (OES) is applied, with the LOS being aligned along the cylinder axis of the quartz tube. The gas temperature T_{gas} is determined after Ref. [32], and the collisional-radiative model `Yacora` is used for the evaluation of the electron density n_e, electron temperature T_e and atomic hydrogen density n_H [14, 33]. Since H_3^+ is the dominant ion at the present setup, the mean ion mass is approximated by $m_i \approx 3$ u [34, 35].

In Table 1, the determined plasma parameters and corresponding VUV, atom and positive ion fluxes leaving the plasma volume of the external plasma source are listed. The applied operational parameters for the external plasma source are 10 Pa/400 W and 4 Pa/600 W within this work. To calculate the fluxes reaching the caesiated sample surface from the fluxes leaving the plasma volume, ballistic propagation with isotropic emission from the open front end surface A_p of the quartz tube is assumed and the divergence into the main chamber is taken into account. To do so, the solid angle $d\Omega_{spl} = dA_{spl}\cos(\beta)/s^2$ of a surface element dA_{spl} on the caesiated sample surface with respect to A_p is considered, where $\beta = 45\,^\circ$ is the angle between the normal of A_p and the normal of dA_{spl}, and s is the distance between dA_{spl} and the position on A_p. With θ being the angle between the direction of the emitted species and the normal of A_p, the factor [36]

$$F_\Omega = \frac{1}{2\pi}\int_{\tilde{A}_p} \cos(\theta)\frac{\cos(\beta)}{s^2}\mathrm{d}A \tag{3}$$

is calculated, which is multiplied with the fluxes given in Table 1. For the integration in Eq. (3) it needs to be taken into account that the flange to which the external plasma source is connected limits the emitting area A_p from which plasma species can reach dA_{spl} and that the area on the caesiated surface that needs to be considered is the spot where the work function is monitored (diameter $\approx$ 15 mm). This leads to a reduced emitting area $\tilde{A}_p$ and to $F_\Omega = 2.3 \times 10^{-3}$.

Since the gas pressure in the vacuum system is several Pa during the operation of the source, the plasma species inevitably interact with particles on the way toward the caesiated surface. In the case of photons, reabsorption processes can occur that attenuate the radiation. Such effects are, however, intrinsically considered in the measurement with the VUV diagnostic, as the device is installed at a distance that is comparable with the distance to the sample holder. In the case of hydrogen atoms and ions, collisional processes are expected to reduce the particle fluxes. Moreover, the evolution of the electrical potential from the external plasma source toward the main chamber that is decisive for the resulting ion flux is unknown. While unfortunately no diagnostic for the detection of hydrogen atoms propagating toward the sample holder is available, the ions can be measured with a

Table 1 Plasma parameters as well as VUV, atom and positive ion fluxes of hydrogen discharges generated in the external plasma source (EPS) and internal plasma source (IPS) at ACCesS at standard operational parameters

	EPS 10 Pa/400 W	EPS 4 Pa/600 W	IPS 10 Pa/250 W
T_{gas} / K	662	656	550
n_e / m^{-3}	6.9×10^{16}	4.3×10^{16}	1.4×10^{16}
T_e / eV	4.4	7.9	2.1
n_H / m^{-3}	2.8×10^{20}	1.0×10^{20}	1.7×10^{19}
Γ_{VUV} / m^{-2}s^{-1}	3.4×10^{20}	8.5×10^{20}	4.2×10^{19}
Γ_H / m^{-2}s^{-1}	2.6×10^{23}	9.3×10^{22}	1.4×10^{22}
$\Gamma_{H_3^+}$ / m^{-2}s^{-1}	4.1×10^{20}	3.4×10^{20}	1.2×10^{20}

Langmuir probe at the setup. The Langmuir probe is installed at the radial flange opposite to the external plasma source and inserted into the main chamber until the probe tip reaches the flange to which the external plasma source is connected (sample holder being removed from the experiment). By moving the Langmuir probe from the flange toward the position of the sample surface in the main chamber, ion fluxes are determined from the measured ion currents as a function of the distance to the flange. The determined ion fluxes decrease with increasing distance to the flange and the decrease is more pronounced at 10 Pa than at 4 Pa, which is attributed to a higher collision rate. Unfortunately, the lower detection limit of the Langmuir probe system is reached at 10 Pa at a distance of about 3 cm and at 4 Pa at a distance of about 1 cm from the sample surface position, which means that the ion flux cannot be determined directly at the position of the sample surface with the Langmuir probe. The measured ion fluxes with the Langmuir probe are comparable to those calculated by assuming ballistic propagation, but it needs to be considered that the ions are collected from a certain volume around the probe tip, meaning that upper limits for the actual fluxes are determined. Hence, it is evidently confirmed that the calculated ion fluxes are upper limits. It is expected that the same is valid for the atomic hydrogen flux.

The bar diagram in Fig. 2 summarizes the calculated fluxes onto the caesiated surface from the external plasma source. The different contributions from the VUV range are represented as stacked bars, and the facts that the particle fluxes represent upper limits and that the actual particle fluxes are further below the upper limit at 10 Pa than at 4 Pa are indicated by the dashed upper parts of the bars and the vertical arrows with different lengths, respectively.

In addition, the fluxes onto the caesiated surface from hydrogen discharges that are ignited in the main chamber (called internal plasma source in the following) are depicted in Fig. 2. The applied operational parameters for the internal plasma source are 10 Pa/250 W. The corresponding plasma parameters are listed in Table 1, where T_{gas} and n_H are determined via OES by using the LOS usually foreseen for TDLAS (see Fig. 1). T_e and n_e are

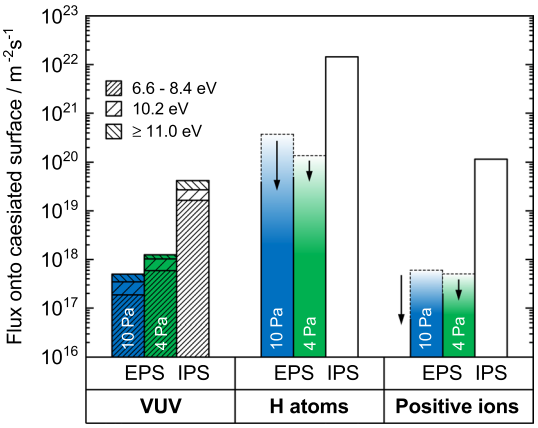

Fig. 2 VUV, atom and positive ion fluxes onto the caesiated surface from hydrogen discharges generated in the external plasma source (EPS) at 10 Pa/400 W (in blue) and 4 Pa/600 W (in green), and in the internal plasma source (IPS) at 10 Pa/250 W. The VUV fluxes are plotted as stacked bars, showing the contributions from different energy ranges. The particle fluxes from the EPS are calculated assuming ballistic transport, meaning that the plotted values represent upper limits and the actual fluxes reaching the surface decrease with increasing pressure, indicated by the dotted upper parts of the bars and the arrows with different lengths

measured with the Langmuir probe, which in this case is installed at the flange behind the sample holder and is fed through the sample holder to measure the plasma parameters directly above the sample surface (see [25]). The maximum energy of the positive ions striking the surface is determined from the difference between the plasma potential and the floating potential of the surface and is about 8 eV, i.e., the VUV photons are the most energetic species. The VUV fluxes are measured with the VUV diagnostic, which is installed at the main chamber for these measurements (for details see [31]). In general, the fluxes in the full plasma-surface interaction are (more than) two orders of magnitude higher than the ones from the external plasma source and are comparable to the ones close to the extraction system at negative hydrogen ion sources for fusion [14].

Results and Discussion

To ensure reproducibility, the Mo substrates used within this work are prepared as follows: They are cleaned with distilled water and isopropyl alcohol and are installed at the sample holder after cleaning the experimental chamber to remove Cs and Cs compounds from previous campaigns. Then, a hydrogen plasma is generated in the main chamber (internal plasma source) for a couple of hours to remove adsorbed impurities from ambient air from the Mo surface via the plasma-surface interaction and the plasma induced temperature increase to ≈ 220 °C. The surface work function measured after this procedure lies reproducibly above 4 eV, which is in accordance with literature values [4–6]. Cs is evaporated into the chamber after the surface has cooled to room temperature, and the neutral Cs density is continuously monitored via TDLAS. To generate ultra-low work function layers with a work function of 1.25 ± 0.10 eV, the Cs density is ramped up to $\sim 10^{15}$ m^{-3}. This results in a flux ratio of Cs to residual H_2O of $\Gamma_{Cs}/\Gamma_{H_2O} \sim 5 \times 10^{-3}$ ($\Gamma_{Cs} \approx 5 \times 10^{16}$ m^{-2}s^{-1}, $\Gamma_{H_2O} \approx 1 \times 10^{19}$ m^{-2}s^{-1}), which is found to be the minimum required to achieve the ultra-low work function [20]. The ultra-low work function is attributed to the formation of Cs oxides from the interaction of Cs and H_2O on the surface [19]. The work function remains stable as long as the Cs density is sustained above 10^{15} m^{-3}, and it is not affected by hydrogen gas up to several Pa [20].

When the Cs evaporation is stopped and the sample is left in vacuum, the moderate vacuum conditions lead to an increase in the work function to $2.6 - 2.7$ eV on the hour scale and to about 2.8 eV the next day. In the subsequent days, work functions higher than 3 eV are obtained. The increase in the work function shows that the Cs layer gradually degrades, which is explained by the continuous accumulation of residual gases, changing the chemical composition and stoichiometry at the surface. In consequence, degraded Cs layers need to be reactivated after operational breaks in order to regain (ultra-)low work function values.

Degraded Cs Layers

Exposure to VUV Photons

To investigate the impact of energetic VUV photons on degraded Cs layers, the MgF_2 window is applied as described in Sec. 2.1. The external plasma source is operated at

10 Pa/400 W, providing the VUV fluxes shown in Fig. 2. By taking the transmission of the MgF_2 window into account, the resulting photon flux onto the surface is 2.8×10^{17} $m^{-2}s^{-1}$ with energies $\lesssim 11.0$ eV.

In Fig. 3a, the influence of the photon irradiation on the work function of Cs layers in different degradation states is presented. The work function is plotted as a function of the cumulative irradiation time (bottom x-axis) and as a function of the corresponding VUV fluence (top x-axis), the latter being the time integrated VUV flux the surface is exposed to (in units of m^{-2}). As can be seen, the photon irradiation leads to a significant reduction in the work function. For an initial work function of 3.0 eV (plotted in black), an irradiation time of 30 s leads to a reduction to 2.7 eV, and for cumulative irradiation times up to 11 min, the work function remains in the range of 2.7 ± 0.1 eV. For longer irradiation times, a further reduction to about 2.5 eV is obtained. When the initial work functions are 3.2 and 3.3 eV (blue and green curves), an irradiation time of 30 s also leads to a work function of 2.7 eV, and in the case the Cs layer is heavily degraded to a work function of 3.8 eV after four weeks (red curve), an about three times longer irradiation time is needed to reach 2.7 eV. A further reduction to 2.5 eV is, however, not observed for initial work functions > 3 eV, even for applied cumulative irradiation times up to 5 h. Since the temperature of the surface remains constant at room temperature during the experiments, thermal effects can be disregarded. Cs is not detected with the TDLAS system during the irradiation, showing that no significant Cs desorption from the surface is induced.

Although the same work function of 2.7 eV is evaluated within the error bars after the photon irradiation of Cs layers in different degradation states, the QE of the surface can differ significantly, showing that the surface condition after the irradiation still depends on the history of the sample. The reached QE is typically higher the lower the initial work function, which is demonstrated for a photon energy of 3.1 eV in Fig. 3b.

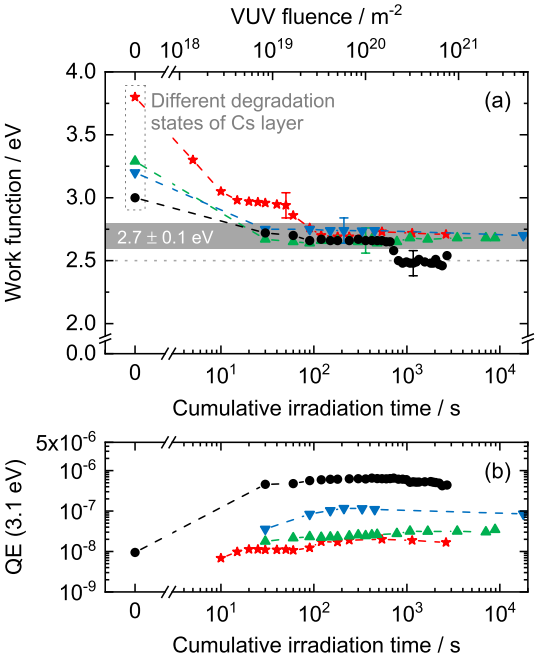

Fig. 3 **a** Work function evolution of Cs layers on Mo in different degradation states upon irradiation with photons up to 11 eV. **b** Corresponding QE progressions at 3.1 eV

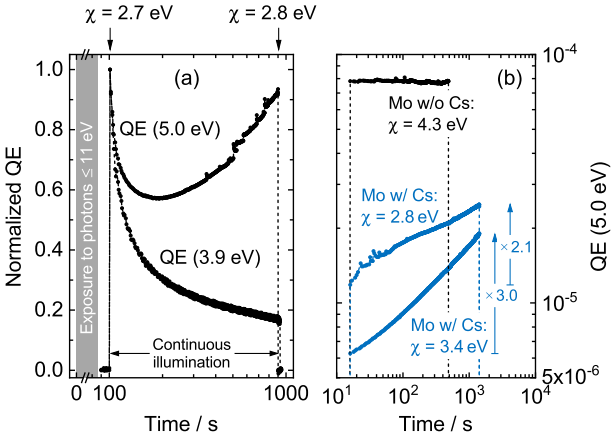

Fig. 4 **a** Typical evolution of the QE at 3.9 and 5.0 eV shortly after irradiating degraded Cs layers on Mo with photons up to 11 eV. **b** Evolution of the QE at 5.0 eV of an uncaesiated Mo surface and of caesiated Mo surfaces in different degradation states

In addition, the QE after the photon irradiation shows a strong temporal dynamic. In Fig. 4a, the typical temporal behavior of the QE within the first minutes after the irradiation from the external plasma source is demonstrated, with the retrieved work function being 2.7 eV. The depicted QE(3.9 eV) and QE(5.0 eV) measurements are taken by continuous illumination with 3.9 and 5.0 eV photons (in different experiments) by using the mercury lamp of the work function diagnostic with the respective interference filters. The corresponding photon fluxes onto the surface are 8×10^{18} $m^{-2}s^{-1}$ for 3.9 eV and 3×10^{18} m^{-2} s^{-1} for 5.0 eV, i.e., the photon fluxes are higher than the VUV flux from the external plasma source. The measured QEs are normalized to the respective values measured right at the beginning of the illumination. In the case of QE(3.9 eV), a continuous decrease can be observed. The QE is reduced by 50% after 25 s and by 83% after about 14 min, showing that the surface is subject to a substantial degradation. The measured work function afterward is 2.8 eV, i.e., the work function increases by about 0.1 eV during the illumination period. Since for photon energies below 3.9 eV the temporal behavior of the QE is comparable (not shown), the QE(3.1 eV) values plotted in Fig. 3b represent a "snapshot", taken ≈ 90 s after the termination of the irradiation from the external plasma source. In the case of QE(5.0 eV) in Fig. 4a, the decrease within the first seconds of illumination is similar to QE(3.9 eV). However, the decrease slows down and after about 1.5 min during which the QE is reduced by 43%, the QE starts to increase again. At the end of the illumination period of 14 min, the QE(5.0 eV) yields 93% of the initially measured value. The measured work function afterward is 2.8 eV, which is the same as after the illumination with 3.9 eV photons.

When degraded Cs layers are irradiated with 5.0 eV photons without prior photon irradiation from the external plasma source, the respective QE gradually increases without initially decreasing. This is demonstrated in Fig. 4b, where during an irradiation time of 23 min the QE(5.0 eV) values of Cs layers with work functions of 2.8 and 3.4 eV increase by a factor of 2.1 and 3.0, respectively. Remarkably, the QE(5.0 eV) values of the degraded Cs layers are up to an order of magnitude lower than the QE(5.0 eV) of an uncaesiated Mo surface with a work function of 4.3 eV, where the QE remains stable over the irradiation period as expected. The lower QE despite the lower work function can be explained by a lower electron density at the surface, as the Fermi energy of Cs (1.59 eV [6]) is low compared to the Fermi energy of Mo (6.77 eV [37]). In addition, the electron escape depth is

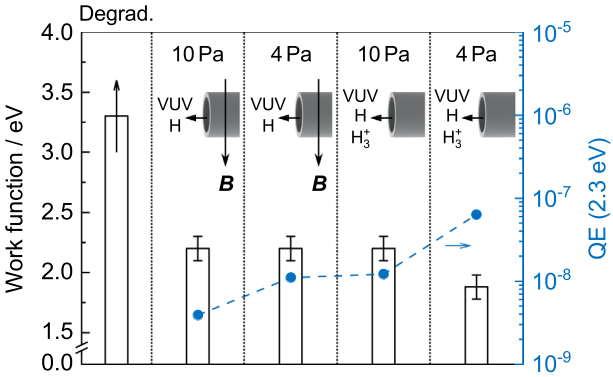

Fig. 5 Work function reduction of degraded Cs layers on Mo upon exposure to hydrogen plasma species with and without positive ions. The external plasma source is operated at 10 Pa/400 W and 4 Pa/600 W. Typical QEs at 2.3 eV are depicted

only $\sim 1-10$ nm [38] and the penetration depth of the energetic photons is much longer in Cs ($\sim$ 100 nm [39]) than in Mo ($\sim$ 10 nm [40, 41]), meaning that in the case of thick Cs layers a significant amount of photoelectrons might not reach the surface [42]. Both in Fig. 4a and b, the increase in the QE upon the irradiation with 5.0 eV photons is attributed to photo-induced changes of the surface. A reduction in the work function after the irradiation with 5.0 eV photons is, however, not observed. Therefore, the work function decrease after the photon irradiation from the external plasma source shown in Fig. 3 is attributed to the VUV photons with energies higher than 5 and up to 11 eV, even if their flux is more than one order of magnitude lower. It is suggested that the VUV photons effectively dissociate Cs compounds (e.g., CsOH) and residual gas molecules (mainly H_2O) at the surface, leading to a significant change of the chemical composition of the surface. Moreover, photo-induced desorption processes might play a role.

Exposure to VUV Photons, Hydrogen Atoms and Positive Ions

In order to study the work function change of degraded Cs layers upon VUV irradiation together with hydrogen atoms with and without positive ions, the external plasma source is operated both at 10 Pa/400 W and 4 Pa/600 W to change the particle fluxes onto the surface. Similar to the investigations described above, Cs layers in different degradation states are prepared. When the source is operated at 10 Pa/400 W and the positive ions are suppressed by the magnetic filter, the work function is reduced to 2.2 eV after a cumulative irradiation time of about 1 min. The corresponding VUV fluence is $\sim 3 \times 10^{19}$ m^{-2}, with which in the case of pure photon irradiation a work function of 2.7 eV is obtained (see Fig. 3). As already mentioned, the energy range of the photons striking the surface is extended from 11 to about 15 eV without the MgF_2 window. However, it is assumed that the higher photon energy of the additional photon flux plays a subordinate role, as the dissociation energies of Cs compounds and residual gas molecules as well as typical adsorption energies are well below 11 eV [6]. The enhanced work function reduction is thus attributed to the additional impact of the atomic hydrogen radicals. The cumulative irradiation time is extended up to 3 h and the work function remains constant in the range of 2.2 ± 0.1 eV. Similar to the case of pure photon irradiation the reached QE is systematically lower the higher the initial work function, showing that the retrieved surface properties still depend on the previous degradation state.

As shown in Fig. 5, the work function is also reduced to 2.2 ± 0.1 eV when the external plasma source is operated at 4 Pa/600 W, i.e., at a presumably higher H atom flux and a higher VUV flux by a factor of 2.5 (see discussion in Sec. 2.2 and Fig. 2). When the magnetic filter is removed at 10 Pa, the obtained work function is still 2.2 eV, but in the case of 4 Pa, a further reduction to 1.9 eV is achieved. In all cases, the work function reduction occurs on the time scale of minutes.

Additionally depicted in Fig. 5 are the typical QEs at 2.3 eV (close to the work function). The QE(2.3 eV) increases by about half an order of magnitude when the pressure is reduced from 10 to 4 Pa with magnetic filter, which is attributed to the higher expected atomic flux and the higher VUV flux. At 10 Pa without magnetic filter, the QE is comparable to the one at 4 Pa with magnetic filter because the lower H and VUV fluxes are presumably compensated by positive ions striking the surface. At 4 Pa without magnetic filter, the fluxes are expected to be the largest, leading to the highest QE and the lowest work function.

The selective exposure reveals that VUV, atom and ion fluxes are beneficial to reactivate degraded Cs layers to some extent. Since the temperature of the surface increases only by a few degrees during the irradiation, thermal effects can be neglected. Furthermore, Cs is not detected with the TDLAS system, implying that Cs is not redistributed within the experiment and the removal of Cs from the surface is inefficient at the given fluxes. In consequence, changes of the chemical composition of the surface are driven by photochemical processes and interactions with hydrogen atoms and ions.

Exposure to Full Plasma-Surface Interaction

To investigate the work function behavior of degraded Cs layers upon full plasma-surface interaction, plasma pulses of a few seconds are applied in the ACCesS main chamber (internal plasma source) and the work function is measured afterward. The minimum work function achieved by this is 1.9 ± 0.1 eV and is given after a cumulative plasma-on time of the order of 10 s. The reached work function as well as QEs are comparable to the ones achieved during the irradiation with photons, hydrogen atoms and ions from the external plasma source (see Fig. 5), indicating that the induced chemical reactions at the surface and resulting modifications of the chemical composition are similar. This result is remarkable because the applied fluxes and fluences are orders of magnitude higher for the plasma ignition in front of the surface than from the external plasma source (see Fig. 2). Depending on the total amount of Cs that was evaporated into the chamber (experimental history), the measured neutral Cs density during the pulses is in the range of $10^{14} - 10^{16}$ m^{-3} and instantly drops below the detection limit when the plasma is switched off (note that ionized Cs and Cs compounds are not detected). Hence, a considerable Cs redistribution is driven within the experiment without having a significant influence on the resulting work function of the surface. As the temperature of the chamber walls is about 22 °C (water-cooled) and the temperature of the sample surface remains below 50 °C, thermal desorption of Cs from the surfaces can be neglected and the Cs release is mainly attributed to chemical sputtering [25]. During the first pulses an increase in the signals for H_2O, N_2 and CO_2 is observed in the RGA recording, showing that adsorbed residual gases within the experiment are released as well.

Investigations with various degraded Cs layers in different campaigns reveal that the achieved work function can be $0.1 - 0.2$ eV higher than 1.9 eV. However, no clear relationship between the initial work function/experimental history and the achieved work function

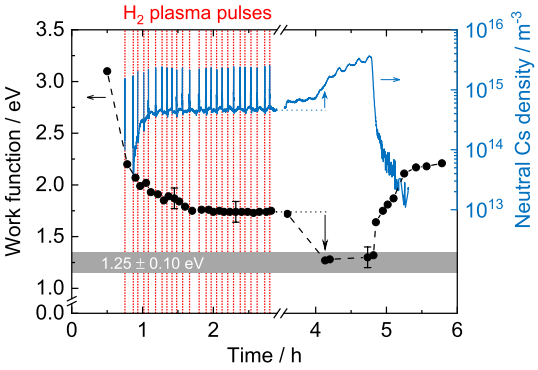

Fig. 6 Work function evolution of a degraded Cs layer on Mo upon the exposure to repetitive 5 s hydrogen plasma pulses (indicated by the dotted vertical red lines) together with Cs evaporation. The continuously monitored neutral Cs density is depicted

minimum is identified. Therefore, it can be stated that a reproducible conditioning of degraded Cs layers is not achieved by the application of short plasma pulses. By extending the cumulative plasma-on time from minutes to hours, the work function starts to increase after some time due to the gradual removal of Cs from the surface [25].

As described in Ref. [20], the minimum work function that is typically achieved by re-caesiation of degraded Cs layers without plasma exposure is $1.9 - 2.1$ eV. When plasma pulses are applied together with re-caesiation, however, a beneficial synergistic effect is revealed as a further reduction in the work function is observed. This is demonstrated in Fig. 6, where hydrogen plasma pulses of 5 s are repetitively applied together with continuous Cs evaporation. The duration of vacuum phases in between plasma pulses is $3 - 5$ min during which the work function is measured. The initial work function of 3.1 eV is reduced to 2.2 eV by the first pulse, with the measured neutral Cs density being slightly above 10^{15} m^{-3}. After the subsequent pulse the work function is 2.1 eV and the Cs evaporation is started. The evaporation rate is gradually increased, leading to a Cs density of $\sim 5 \times 10^{14}$ m^{-3} during vacuum and $\sim 2 \times 10^{15}$ m^{-3} during plasma phases. The work function decreases below 1.9 eV and reaches a stable plateau of 1.75 ± 0.10 eV after a plasma-on time of 1 min (surface temperature below 50 °C). After the application of 25 pulses the Cs density is maintained and the work function remains constant. When the Cs density is increased to $\gtrsim 10^{15}$ m^{-3} in the following, the work function decreases to ultra-low values of 1.3 eV.

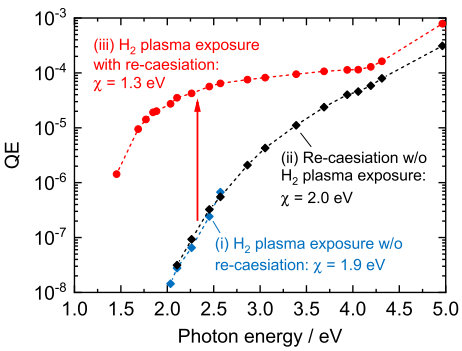

Fig. 7 Typical QE curves of caesiated Mo surfaces measured after the reactivation of degraded Cs layers with (i) short hydrogen plasma pulses, (ii) re-caesiation, and (iii) the combination of both. Evaluated work functions from the measured QE curves are given

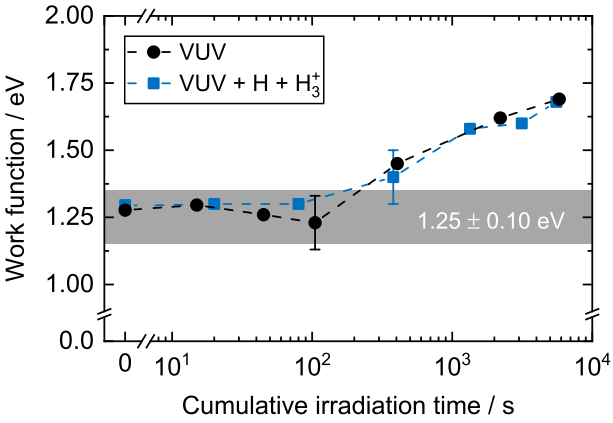

Fig. 8 Work function behavior of caesiated Mo surfaces with initial $\chi = 1.25 \pm 0.10$ eV during Cs evaporation together with VUV irradiation (energies up to 11 eV) and together with VUV, hydrogen atom and positive ion exposure. The neutral Cs density above the sample surface is maintained at $\sim 10^{15}$ m^{-3} during both experiments

Further investigations have shown that the exposure of degraded Cs layers to a series of hydrogen plasma pulses of a few seconds in combination with stable Cs densities $\gtrsim 10^{15}$ m^{-3} in the vacuum phase leads to a reliable retrieval of work functions in the range of 1.25 ± 0.10 eV. In general, the ultra-low work function is retrieved faster the weaker the degradation. However, for a detailed evaluation of the dependence of the temporal work function evolution on the initial degradation state and number of plasma pulses required further studies would be necessary.

In Fig. 7, typical QE curves corresponding to the application of (i) plasma pulses without re-caesiation ($\chi = 1.9$ eV), (ii) re-caesiation without plasma pulses ($\chi = 2.0$ eV), and (iii) plasma pulses together with re-caesiation ($\chi = 1.3$ eV) are plotted. While the scenarios (i) and (ii) lead to comparable QEs in the energy range of $2.1 - 2.6$ eV, a $2 - 3$ orders of magnitude higher QE is achieved in (iii), where the photoelectric response is extended to the near IR. Apart from the lower work function, the higher QE of the surface is also expected to be beneficial for the negative ion production, as it indicates a higher electron density at the surface [7]. Since the work function of 1.3 eV is only reached when the Cs density is $\gtrsim 10^{15}$ m^{-3} (see Fig. 6), the flux ratio of Cs to residual H_2O still seems to be decisive to grow ultra-low work function layers.

Ultra-Low Work Function Layers

Exposure to VUV Photons

Similar to the investigations described in Sec. 3.1, ultra-low work function layers are exposed to VUV radiation from the external plasma source (operated at 10 Pa/400 W) by applying the MgF_2 window. The neutral Cs density in the main chamber is kept at $\sim 10^{15}$ m^{-3} during the experiments, which is the requirement for stable ultra-low work function layers in vacuum [20]. As shown in Fig. 8, the work function is stable at 1.25 ± 0.10 eV for irradiation times up to about 2 min, but increases for longer irradiation times, corresponding to VUV fluences $\gtrsim 10^{20}$ m^{-2}. After about 1.5 h (VUV fluence $\sim 10^{21}$ m^{-2}), a significantly increased work function of 1.7 eV is obtained despite the still constant Cs influx. When Cs layers with a work function of 1.25 eV are exposed to comparable fluences with 5.0 eV photons from the mercury lamp (cp. Fig. 4), no influence on the work function can be detected (not shown). Therefore, the increase in the work function

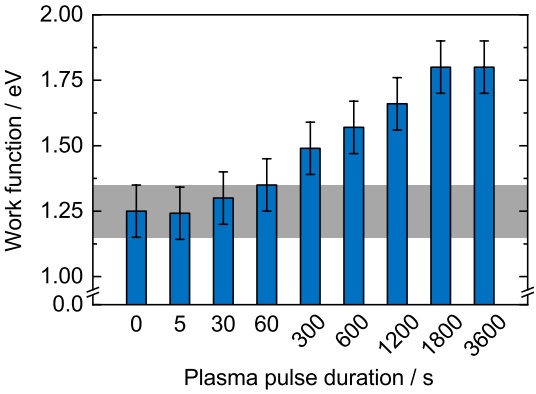

Fig. 9 Work function after the exposure of caesiated Mo surfaces with initial $\chi = 1.25 \pm 0.10$ eV to different hydrogen plasma pulse durations. The neutral Cs density is $\sim 10^{15}$ m^{-3} during the vacuum phase and in the range of $10^{15} - 10^{16}$ m^{-3} during the plasma pulse

is attributed to changes of the surface induced by photons with energies of 5 to 11 eV. A plausible reason for the work function increase is the photolysis of Cs compounds (in particular Cs oxides) at the surface.

After the VUV irradiation is stopped, the ultra-low work function can be regained within several minutes. Hence, changes of the chemical composition of the surface upon VUV irradiation are reversible.

Exposure to VUV Photons, Hydrogen Atoms and Positive Ions

When the ultra-low work function surface is exposed to VUV photons together with hydrogen atoms and positive hydrogen ions (no MgF_2 or magnetic filter applied), the work function evolution is quite similar to the one resulting from photon irradiation only. As can be seen in Fig. 8, the work function increases up to ≈ 1.7 eV for irradiation times exceeding a few minutes. Consequently, the governing processes that are responsible for the increase in the work function are expected to be photochemical reactions, and atomic and ionic particles seem to play a subordinate role here. After the irradiation with the plasma species is stopped, the ultra-low work function is retrieved within a couple of minutes, again comparable to the situation of photon irradiation only.

Exposure to Full Plasma-Surface Interaction

Plasma pulses with different pulse durations are applied with the internal plasma source to investigate the durability of ultra-low work function layers upon full plasma-surface interaction. The neutral Cs density is $\sim 10^{15}$ m^{-3} during the vacuum phase to generate and maintain the ultra-low work function. During the plasma pulses, the neutral Cs density is increased and in the range of $10^{15} - 10^{16}$ m^{-3} due to the plasma-induced Cs redistribution within the chamber. The bar diagram in Fig. 9 presents the work functions measured after the different applied plasma pulse durations. Up to about 1 min, the work function remains in the range of 1.25 ± 0.10 eV. The corresponding VUV fluence for pulses of 1 min is of the order of 10^{21} m^{-2}, with which with VUV irradiation from the external plasma source an increase in the work function is observed. Possible reasons for the enhanced durability might be the elevated Cs density during the plasma phase and/or the redistribution of Cs compounds within the chamber. For longer

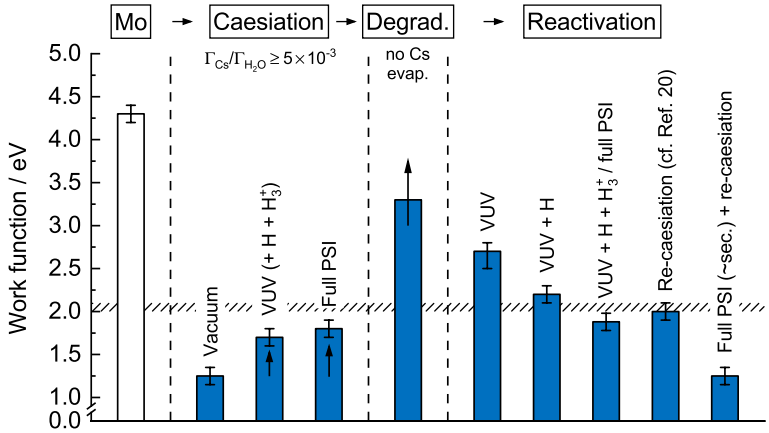

Fig. 10 Work function dynamics of ultra-low work function and degraded Cs layers upon exposure to specific hydrogen plasma species and full plasma-surface interaction (PSI). The applied plasma species fluxes are provided in Fig. 2 and the work function of bulk Cs is indicated as dashed horizontal bar

exposure times, however, the work function increases, which shows that the ultra-low work function layer is not stable in the hydrogen plasma environment. After about half an hour of continuous plasma exposure, the surface temperature is 220 °C and the work function reaches a stable plateau of 1.8 ± 0.1 eV. Since it is shown in [43] that Cs oxide coatings are stable for temperatures up to ~ 200 °C, it is suggested that thermal effects play a subordinate role here and the increase in the work function is mainly driven by physico-chemical interactions with the impinging plasma species.

After the plasma exposure is stopped, the work function decreases again and ultra-low values are retrieved. The time it takes for the retrieval of the ultra-low values is shorter the less the work function has increased, i.e., the recovery time depends on the applied plasma pulse duration. In general, the retrieval of $1.2 - 1.3$ eV occurs on a time scale comparable to the plasma pulse duration.

Compilation of Work Function Dynamics

The conducted experiments impressively demonstrate that caesiated surfaces are heavily influenced by the interaction with hydrogen plasma species. The influence depends on the exposure time and initial surface condition and can range from a decrease to an increase in the work function as summarized in Fig. 10. Ultra-low work functions of 1.25 ± 0.10 eV, which are generated with a Cs to H_2O flux ratio of $\gtrsim 5 \times 10^{-3}$ onto the surface, are sustained upon plasma exposure times $\lesssim 1$ min (applied plasma parameters given in Table 1). For longer exposure times, the work function increases. The increase is mainly attributed to the VUV irradiation, which is inevitably present in the hydrogen plasma environment. It was shown that the exposure to VUV photons with energies of $5 - 11$ eV cause a gradual increase in the work function and lead to 1.7 eV for a VUV fluence of the order of 10^{21} m^{-2} while maintaining the Cs to H_2O flux ratio constant. Hence, photochemical reactions (e.g., photolysis of Cs oxides) change the chemical composition of the surface considerably and play an important role in the plasma-surface interaction.

The work function that is reached upon steady-state plasma exposure is 1.8 ± 0.1 eV, which is above the ultra-low regime but still lower than the work function of bulk Cs. The

work function of 1.8 eV is stable for plasma exposure times of several hours, where the neutral Cs density is kept in the range of $10^{15} - 10^{16}$ m^{-3}. Hence, the Cs flux onto the surface and plasma-induced Cs release from the surface are in balance and an equilibrium surface state is reached. When the Cs flux onto the surface is too low during plasma exposure, the work function gets unstable and gradually increases above 1.8 eV due to the depletion of Cs (compounds) at the surface. At the present setup this is the case for neutral Cs densities $\lesssim 3 \times 10^{14}$ m^{-3}, corresponding to neutral Cs fluxes $\lesssim 2 \times 10^{16}$ m^{-2}s^{-1}.

When the Cs evaporation is stopped and the caesiated surface is left in vacuum, the work function gradually increases due to the influx of residual gases. With the present background pressure of some 10^{-6} mbar a work function of 2.8 eV is given after half a day, and values higher than 3 eV are obtained after several days. This degradation can partly be reversed by the interaction with hydrogen plasma species. VUV photons with energies of $5 - 11$ eV lead to $2.8 - 2.5$ eV for fluences of the order of 10^{20} m^{-2}. By the addition of hydrogen atoms, a further decrease to 2.2 eV is obtained, and in the case of VUV photons together with hydrogen atoms and positive ions a value of 1.9 eV is achieved in minimum, which is also obtained with full plasma exposure. Hence, the plasma species modify the chemical composition of degraded Cs layers and can lead to a work function reduction of more than 1 eV. However, it needs to be taken into account that the more the surface is degraded, the lower the retrieved QE of the surface. A higher QE is generally expected to be beneficial for the production of negative hydrogen ions, as it indicates a higher electron density at the surface.

The retrieval of ultra-low work functions from degraded Cs layers is not achieved by plasma exposure without re-caesiation nor by re-caesiation without plasma exposure (minimum work function in both cases in the range of $1.9 - 2.1$ eV). However, by the application of short repetitive plasma pulses (of the order of seconds) in combination with continuous Cs evaporation, ultra-low work functions in the range of 1.25 ± 0.10 eV are regained, provided that the required Cs to H_2O flux ratio is given. The retrieval of the ultra-low work function is accompanied by a significant enhancement of the QE and reveals a beneficial synergistic effect of hydrogen plasma treatment and fresh Cs adsorption.

Conclusions

The usage of Cs introduces temporal dynamics in the operation of negative hydrogen ion sources because the plasma-surface interaction leads to the redistribution of Cs and affects the work function of the converter surface considerably. By the selective exposure of caesiated surfaces to hydrogen plasma species it is shown for the first time that VUV photons (up to 11 eV) lead to changes of the surface composition and that hydrogen atoms and positive hydrogen ions can affect the surface separately. Therefore, photonic, atomic as well as ionic interactions lead to work function changes and must be considered in the plasma-surface interaction. The work function is decisive for the extracted negative ion current as well as for the co-extracted electron current, the latter often limiting the ion source performance.

Due to the passivation of caesiated surfaces in the absence of Cs evaporation, a Cs conditioning procedure is required after operational breaks to reduce the work function of the converter surface and to approach the optimum source performance. By the application of plasma pulses without Cs evaporation or re-caesiation without plasma pulses the achieved work function minimum is in the range of $1.9 - 2.1$ eV. In order to obtain ultra-low work

functions in the range of $1.2 - 1.3$ eV, the application of repetitive plasma pulses in combination with continuous Cs evaporation is required, which is typically done in ion sources for fusion. The achieved ultra-low work function is attributed to the formation of Cs oxides at the surface due to reactions between Cs and residual H_2O, and is obtained for a Cs to H_2O flux ratio of $\gtrsim 5 \times 10^{-3}$.

Cs layers with a work function of $1.2 - 1.3$ eV withstand plasma pulse durations of $\lesssim 1$ min. For longer plasma exposure times, however, a gradual increase in the work function is obtained and a stable value of 1.8 ± 0.1 eV is reached in steady-state for a sufficiently high Cs flux onto the surface. The application of long pulses at ion sources (several minutes up to one hour) is typically accompanied by a deterioration of the source performance over time, which shows up first by an increase in the co-extracted electron current before ultimately also the extracted negative ion current decreases. This temporal behavior could consequently be explained by the gradual increase in the work function above the ultra-low regime.

After the application of long pulses, the ion source performance is typically recovered within vacuum breaks of several minutes during which Cs is continuously evaporated. Since the plasma impact does not lead to irreversible effects and ultra-low work functions are retrieved during vacuum phases of several minutes, the recovery of the ion source performance can be explained by the re-establishment of an ultra-low work function coating on the converter surface. Consequently, the continuous evaporation of Cs during vacuum phases is highly beneficial for the preparation of long pulses.

Since it is found that the work function of ultra-low work function layers increases by about 0.5 eV upon VUV irradiation despite keeping the Cs flux in the desired range, a temporal increase in the converter work function and the associated deterioration of the optimum ion source performance seem to be unavoidable during long pulses due to the inevitable presence of VUV photons in a hydrogen plasma environment. To minimize the increase in the work function, the focus should be laid on the stabilization of Cs oxides at the surface. Future studies will include the application of in situ/operando surface analysis techniques to gain insights into the chemical composition and stoichiometry at the surface. In addition, it should be analyzed to what extent the QE has an impact on the extracted negative ion current and co-extracted electron current. Depending on the operational scenario, the QE of caesiated surfaces can be orders of magnitude different, even for comparable work functions. Since the QE is expected to be correlated with the electron density of the surface, it might be a decisive parameter for the surface production yield of negative hydrogen ions.

Acknowledgements This work has been carried out within the framework of the EUROfusion Consortium, funded by the European Union via the Euratom Research and Training Programme (Grant Agreement No 101052200 - EUROfusion). Views and opinions expressed are, however, those of the authors only and do not necessarily reflect those of the European Union or the European Commission. Neither the European Union nor the European Commission can be held responsible for them.

Author Contributions **Adrian Heiler**: Conceptualization (equal); Data curation (lead); Formal analysis (lead); Investigation (lead); Methodology (equal); Validation (lead); Visualization (lead); Writing—original draft (lead). **Roland Friedl**: Conceptualization (equal); Methodology (equal); Supervision (equal); Writing—review and editing (equal). **Ursel Fantz**: Conceptualization (equal); Supervision (equal); Funding acquisition (lead); Project administration (lead); Writing—review and editing (equal).

Funding Open Access funding enabled and organized by Projekt DEAL.

Data Availability The data that support the findings of this study are available from the corresponding author upon reasonable request.

Declarations

Conflict of interest The authors declare no Conflict of interest.

References

1. Belchenko YI, Dimov GI, Dudnikov VG (1974) A powerful injector of neutrals with a surface-plasma source of negative ions. Nucl Fusion 14:113. https://doi.org/10.1088/0029-5515/14/1/017
2. Fantz U, Lettry J (2018) Focus on sources of negatively charged ions. New J Phys 20:060201. https://doi.org/10.1088/1367-2630/aab317
3. Faircloth D, Lawrie S (2018) An overview of negative hydrogen ion sources for accelerators. New J Phys 20:025007. https://doi.org/10.1088/1367-2630/aaa39e
4. Michaelson HB (1977) The work function of the elements and its periodicity. J Appl Phys 48:4729. https://doi.org/10.1063/1.323539
5. Alton GD (1986) Semi-empirical mathematical relationships for electropositive adsorbate induced work function changes. Surf Sci 175:226. https://doi.org/10.1016/0039-6028(86)90094-4
6. Rumble JR (2022) ed. CRC Handbook of Chemistry and Physics. 103rd. Boca Raton, FL: CRC Press/Taylor & Francis
7. Rasser B, van Wunnik JNM, Los J (1982) Theoretical models of the negative ionization of hydrogen on clean tungsten, cesiated tungsten and cesium surfaces at low energies. Surf Sci 118:697. https://doi.org/10.1016/0039-6028(82)90216-3
8. Wada M, Pyle RV, Stearns JW (1990) Dependence of H production upon the work function of a Mo surface in a cesiated hydrogen discharge. J Appl Phys 67:6334. https://doi.org/10.1063/1.345153
9. Bacal M, Wada M (2015) Negative hydrogen ion production mechanisms. Appl Phys Rev 2:021305. https://doi.org/10.1063/1.4921298
10. Wilson RG (1966) Electron and ion emission from polycrystalline surfaces of Nb, Mo, Ta, W, Re, Os, and Ir in cesium vapor. J Appl Phys 37:4125. https://doi.org/10.1063/1.1707987
11. Swanson LW, Strayer RW (1968) Field-electron-microscopy studies of cesium layers on various refractory metals: work function change. J Chem Phys 48:2421. https://doi.org/10.1063/1.1669464
12. Komppula J et al (2013) VUV-diagnostics of a filament-driven arc discharge H ion source. AIP Conf Proc 1515:66. https://doi.org/10.1063/1.4792771
13. Fantz U et al (2016) Quantification of the VUV radiation in low pressure hydrogen and nitrogen plasmas. Plasma Sources Sci Technol 25:045006. https://doi.org/10.1088/0963-0252/25/4/045006
14. Wünderlich D et al (2021) Emission spectroscopy of negative hydrogen ion sources: from VUV to IR. Rev Sci Instrum 92:123510. https://doi.org/10.1063/5.0075491
15. Friedl R, Fröhler-Bachus C, Fantz U (2024) Determining absolute VUV fluxes for assessing the relevance of photon-surface interaction in ion sources. J Phys Conf Ser 2743:012011. https://doi.org/10.1088/1742-6596/2743/1/012011
16. Mimo A et al (2018) Studies of Cs dynamics in large ion sources using the CsFlow3D code. AIP Conf Proc 2052:040009. https://doi.org/10.1063/1.5083743
17. Wada M (2018) Plasma-surface interaction in negative hydrogen ion sources. Rev Sci Instrum 89:052103. https://doi.org/10.1063/1.5016262
18. Fantz U et al (2024) Contributions of the extended ELISE and BATMAN Upgrade test facilities to the roadmap towards ITER NBI. Nucl Fusion 64:086063. https://doi.org/10.1088/1741-4326/ad5dcd
19. Heiler A, Friedl R, Fantz U (2022) Impact of the photoelectric threshold sensitivity on the work function determination—Revealing ultra-low work functions of caesiated surfaces. AIP Adv 12:035339. https://doi.org/10.1063/5.0078380

20. Heiler A, Friedl R, Fantz U (2024) Ultra-low work function of caesiated surfaces and impact of selected gas species. JINST 19:C01057. https://doi.org/10.1088/1748-0221/19/01/C01057
21. Heiler A et al (2024) Work function of the caesiated converter surface at the BATMAN Upgrade H ion source at different operational scenarios. J Phys Conf Ser 2743:012025. https://doi.org/10.1088/1742-6596/2743/1/012025
22. Fantz U et al (2021) Negative hydrogen ion sources for fusion: from plasma generation to beam properties. Front Phys 9:709651. https://doi.org/10.3389/fphy.2021.709651
23. Wünderlich D et al (2021) NNBI for ITER: status of long pulses in deuterium at the test facilities BATMAN Upgrade and ELISE. Nucl Fusion 61:096023. https://doi.org/10.1088/1741-4326/ac1758
24. Friedl R, Cristofaro S, Fantz U (2018) Work function of Cs-free materials for enhanced H surface production. AIP Conf Proc 2011:050009. https://doi.org/10.1063/1.5053307
25. Cristofaro S, Friedl R, Fantz U (2020) Correlation of Cs flux and work function of a converter surface during long plasma exposure for negative ion sources in view of ITER. Plasma Res Express 2:035009. https://doi.org/10.1088/2516-1067/abae81
26. Heiler A et al (2021) Work function performance of a C12A7 electride surface exposed to low pressure low temperature hydrogen plasmas. J Vac Sci Technol A 39:013002. https://doi.org/10.1116/6.0000749
27. Fowler RH (1931) The analysis of photoelectric sensitivity curves for clean metals at various temperatures. Phys Rev 38:45. https://doi.org/10.1103/PhysRev.38.45
28. Cristofaro S et al (2019) Design and comparison of the Cs ovens for the test facilities ELISE and SPIDER. Rev Sci Instrum 90:113504. https://doi.org/10.1063/1.5128620
29. Fantz U, Wimmer C (2011) Optimizing the laser absorption technique for quantification of caesium densities in negative hydrogen ion sources. J Phys D Appl Phys 44:335202. https://doi.org/10.1088/0022-3727/44/33/335202
30. Wimmer C, Lindauer M, Fantz U (2018) Determination of the Cs distribution along a line of sight by the Zeeman splitting in an inhomogeneous magnetic field. J Phys D Appl Phys 51:395203. https://doi.org/10.1088/1361-6463/aad93d
31. Friedl R, Fröhler-Bachus C, Fantz U (2023) A portable diagnostic system for the quantification of VUV fluxes emitted from low-temperature plasmas. Meas Sci Technol 34:055501. https://doi.org/10.1088/1361-6501/acab23
32. Briefi S, Fantz U (2020) A revised comprehensive approach for determining the H_2 and D_2 rovibrational population from the Fulcher-α emission in low temperature plasmas. Plasma Sources Sci Technol 29:125019. https://doi.org/10.1088/1361-6595/abc085
33. Wünderlich D, Fantz U (2016) Evaluation of state-resolved reaction probabilities and their application in population models for He, H, and H_2. Atoms 4:26. https://doi.org/10.3390/atoms4040026
34. Méndez I et al (2006) Atom and ion chemistry in low pressure hydrogen DC plasmas. J Phys Chem A 110:6060. https://doi.org/10.1021/jp057182+
35. Nunomura S, Kondo M (2007) Characterization of high-pressure capacitively coupled hydrogen plasmas. J Appl Phys 102:093306. https://doi.org/10.1063/1.2809345
36. Kunze H-J (2009) Introduction to plasma spectroscopy. Springer, Berlin, Heidelberg
37. Petroff I, Viswanathan CR (1971) Calculation of density of states in W, Ta, and Mo. Nat. Bur. Stand. (U.S.), Spec. Publ 323:53
38. Seah MP, Dench WA (1979) Quantitative electron spectroscopy of surfaces: a standard data base for electron inelastic mean free paths in solids. Surf Interface Anal 1:2. https://doi.org/10.1002/sia.740010103
39. McWhirter JD (1997) Extinction coefficient and skin depth of alkali metals from 10 to 1000 nm. Opt Lasers Eng 28:305. https://doi.org/10.1016/S0143-8166(97)00018-3
40. Kirillova MM, Nomerovannaya LV, Noskov MM (1971) Optical properties of molybdenum single crystals. Sov Phys JETP 33:1210
41. Preuss S, Demchuk A, Stuke M (1995) Sub-picosecond UV laser ablation of metals. Appl Phys A 61:33. https://doi.org/10.1007/BF01538207
42. Laulainen J et al (2017) Hydrogen plasma induced photoelectron emission from low work function cesium covered metal surfaces. Phys Plasmas 24:103502. https://doi.org/10.1063/1.4998005
43. Melnychuk ST, Seidl M (1991) Reflection of hydrogen atoms from alkali and alkaline earth oxide surfaces. J Vac Sci Technol A 9:1650. https://doi.org/10.1116/1.577480